A Theoretical Study on the Reactions of Hg with Halogens: Atmospheric Implications

Alexei F. Khalizov,*,† Balakrishnan Viswanathan,† Pascal Larregaray,‡ and Parisa A. Ariya†

Departments of Chemistry and Atmospheric and Oceanic Sciences, McGill University, 801 Sherbrooke Street West, Montreal, Quebec, Canada H3A 2K6, and Department of Chemistry and Biochemistry, Concordia University, 1455 de Maisonneuve Boulevard West, Montreal, Quebec, Canada H3G 1M8

Received: April 21, 2003; In Final Form: June 24, 2003

Electronic structure calculations were performed using DFT and high-level ab initio methods to understand the role of atomic halogens in the transformation of gaseous mercury in the Arctic atmosphere. The latter methods were found to be superior in reproducing the reaction enthalpies as well as the geometrical parameters and vibrational frequencies, and therefore they were employed to calculate the energy potentials for the capture−deactivation approach to study the kinetics of halogen−mercury atomic recombination. Using the calculated rate constants and inferred concentrations of halogen atoms in the Arctic troposphere, we found that atomic bromine might be responsible for the mercury depletion episodes.

1. Introduction

Mercury is mainly present in the atmosphere in its elemental form (Hg).[1,2] Its lifetime is of the order of 1−2 years, which provides sufficient time for long-range transport,[2] and explains the observation of nearly uniform mixing ratios of Hg within the Earth's atmosphere.[2] High-temporal-resolution measurements of total gaseous mercury (TGM) in surface air at Alert, Canada, show that TGM concentrations exhibit a large variability in the spring upon the polar sunrise, with frequent episodes of exceedingly low values,[3] which is most unexpected for a species with such a long lifetime. The variability of the mercury concentration is similar in form to the annual pattern of ozone depletion events that occur in the Arctic after the polar sunrise.[4] Moreover, a good positive correlation between the measured concentrations of gaseous mercury and ozone has been observed at this site.[3]

The reactions of Hg with ozone[5−7] and molecular halogens[8−10] are too slow to be a sink of tropospheric Hg. Moreover, these reactions cannot account for the depletion events, as the latter are photochemical in nature, being only observed during the polar sunrise and not during the winter. Photoexcitation of both mercury and ozone can be ruled out since only light with $\lambda >$ 300 nm penetrates the lower troposphere. At the same time, molecular halogens are readily photolyzed at these wavelengths producing halogen atoms, which play an important role in the depletion of ozone in the Arctic.[11−16] Hence, it is very likely that mercury depletion events, having temporal concentration profiles similar to those of ozone, occur through a similar mechanism:

$$X_2 + h\nu \rightarrow 2X \quad (1)$$

$$X + O_3 \rightarrow XO + O_2 \quad (2)$$

$$Hg + X \rightarrow \text{products} \quad (3)$$

$$Hg + XO \rightarrow \text{products} \quad (4)$$

To our knowledge, there is no data on the reactions of mercury with halogen oxides. An evaluation performed using the experimental formation enthalpies shows that the formation of mercury oxide, HgO, and halogen atom, X, in reaction 4 is a thermo-neutral or even moderately exothermic process (from +0.5 to −48.9 kJ mol^{-1}, depending on the nature of X). However, our theoretical computations[17] characterize the above reaction as endothermic to the extent of more than 200 kJ mol^{-1}, due to much lower calculated bonding energy in HgO as compared to experiment. Indeed, in a recent study, using large-scale multireference configuration interaction and coupled cluster calculations on HgO, Shelper and Peterson[18] concluded that gaseous HgO is significantly less stable than currently accepted, and hence it is unlikely that it can be formed directly from the oxidation of Hg by BrO.

While the interaction with halogen atoms seems to be the only plausible process accounting for the fast mercury depletion in the atmosphere, the kinetic data on the reaction of mercury with atomic halogens is scarce.[10,19] In the present work, using high-level DFT and ab initio computations, we performed an extensive study on the structures, vibrational frequencies, and relative energies of the reactants and products involved in the above reactions. Ab initio data were employed in evaluating the reaction rate constants to assess the direct contribution of atomic halogens to the depletion of mercury in the Arctic troposphere.

2. Electronic Structure Calculations

2.1. Computational Methods. Calculations were carried out using the Gaussian 98 (revision A.7) suite of programs.[20] Owing to the large number of electrons and to account for relativistic effects, basis sets with inner electrons substituted by effective core potentials (ECP) were employed for Hg. The first basis set was LanL2DZ, which uses an all-electron description for the first-row elements (D95), and an ECP for inner electrons and double-ζ quality valence functions for the heavier elements.[21−23] The second basis set employs the ECP60MWB pseudopotential of the Stuttgart/Bonn group[24] with the MP2-optimized large uncontracted (9s9p6d4f) Gaussian-type (GTO) valence basis set of Schwerdtfeger and Wesendrup.[25] This yields LanL2DZ and ECP60MWB(9s9p6d4f) basis sets for Hg,

* Author to whom correspondence should be addressed. E-mail address: khalizov@sciborg.uwaterloo.ca.
† McGill University.
‡ Concordia University.

10.1021/jp0350722 CCC: $25.00
Published on Web 07/26/2003

TABLE 1: Calculated Equilibrium Geometries (r_e, Å, degrees) and Harmonic Vibrational Frequencies (cm^{-1}) of HgX and HgX_2 Molecules

species	property	method/basis set: B3LYP/L2	B3LYP/E60&AQZ	QCISD/L2&G6	QCISD/E60&G6	experiment[a] or previous calculations[b]
HgF	r (Hg−F)	2.173	2.076	2.048	2.019	*2.06−2.12*[c−e]
	ω_e	390.3	414.7	486.2	493.2	490.8[f]
HgF_2	r (Hg−F)	2.045	1.932	1.957		1.93[g]
						1.90−2.08[c−e,g−j]
	Σ_g	488.2	564.9	547.7		567.6[k]
	Σ_u	557.6	639.2	619.6		640[k]
	Π_u	82.2	173.8	144.4		170[k]
HgCl	r (Hg−Cl)	2.612	2.455	2.433	2.398	*2.36−2.50*[c−e,l]
	ω_e	228.9	240.0	278.2	278.3	292.6[f]
$HgCl_2$	r (Hg−Cl)	2.442	2.285	2.311		2.33,[m] 2.252,[n]
						2.25−2.44[c−e,g,i,l,o]
	Σ_g	287.7	338.2	328.0		313,[p] 360[q]
	Σ_u	345.1	391.9	376.8		376,[p] 413[q]
	Π_u	66.3	98.2	89.3		100[p]
HgBr	r (Hg−Br)	2.781	2.607	2.580	2.560	*2.60*[c]
	ω_e	141.3	152.7	180.1	173.4	186.5[f]
$HgBr_2$	r (Hg−Br)	2.583	2.423	2.450		2.45,[m] 2.41,[p]
						2.42−2.55[c,g,i]
	Σ_g	177.8	208.0	201.9		195,[p] 225[q]
	Σ_u	243.8	276.3	265.9		271,[p] 293[q]
	Π_u	48.1	65.5	60.5		90[p]

[a] Experimental frequencies are fundamental, ω_e, radii are average, r_0. [b] Results of theoretical calculations are given in *italic*. [c] Ref 31. [d] Ref 32. [e] Ref 33. [f] Ref 40. [g] Ref 30. [h] Ref 34. [i] Ref 35. [j] Ref 36. [k] Ref 56. [l] Ref 37. [m] Ref 57. [n] Ref 39. [o] Ref 38. [p] Ref 58. [q] Ref 59.

denoted as L2 and E60, respectively. For elements O, F, Cl, and Br, we used LanL2DZ, 6-311G(2df), and (aug)-cc-pV*N*Z (N = T, Q, 5, 6)[26−29] basis sets denoted as L2, G6, and (A)NZ, respectively. Geometry optimizations and frequency calculations were performed at the B3LYP and QCISD levels of theory. In the former case, the same basis set was used as for the desired energy calculation; in the latter case, L2&G6 or E60&G6 basis sets were employed for geometry optimization, and then, single-point energy was calculated at the CCSD(T) level using the desired basis set. In correlated ab initio calculations involving bromine, the 3d orbital space was kept frozen.

2.2. Results and Discussion. The reaction of mercury with atomic halogens is known to form HgX intermediates,[19] which may self-react or interact with other atmospheric species. Under atmospheric conditions the self-reaction is too slow to be significant due to the low concentration of HgX. Hence, only reactions with other species, e.g., halogen atoms, were considered in this study:

$$Hg + X \rightarrow HgX \quad (3)$$

$$HgX + X \rightarrow HgX_2 \quad (5)$$

For consistency, the reaction of mercury with molecular halogens was also included:

$$Hg + X_2 \rightarrow HgX_2 \quad (6)$$

The optimized geometries and vibrational frequencies for the HgX and HgX_2 species are presented in Table 1; inter-bond angles are not included because the molecules' equilibrium geometries are always linear. Experimental geometries are available only for mercury dihalides $HgCl_2$ and $HgBr_2$; in the case of HgF_2, the bond length is an estimation made by Cundari[30] using covalent atomic radii and electronegativities. There are no experimental bond lengths for HgX; however, the vibrational frequencies are available. At the same time, a number of theoretical studies report both the geometries and vibrational frequencies of HgX and HgX_2 species calculated at different levels of theory.[30−38] Table 1 shows, where experimental data exist, that in our calculations B3LYP with small LanL2DZ basis set for mercury and halogens overestimated the bond lengths by 0.1 to 0.2 Å and underestimated the vibrational frequencies by 40 to 100 cm^{-1}. Employing larger basis sets, ECP60MWB-(9s9p6d4f) for mercury and aug-cc-pVQZ for halogens, resulted in significantly more accurate bond lengths. Frequencies were well reproduced for closed-shell molecules while for open-shell species they were underestimated by 35 to 75 cm^{-1}. Further extending the basis set for halogens up to aug-cc-pV5Z did not lead to a noticeable change in bond lengths.

Calculations at the QCISD level of theory using either the LanL2DZ or the ECP60MWB(9s9p6d4f) basis set for mercury resulted in quite accurate bond lengths and vibrational frequencies (Table 1); however, for the closed-shell molecules, the latter were better reproduced at the B3LYP level with extended basis set. Using a more extended basis set rather than the moderate 6-311G(2df) in QCISD calculations could have improved the results, but it was too computationally expensive.

Calculated reaction enthalpies $\Delta_r H_{calc}^{298}$ are presented in Table 2 as deviations from "experimental" values, $\Delta_r H_{exp}^{298}$; the latter were derived from the tabulated experimental enthalpies of formation, $\Delta_f H_{exp}^{298}$, of the corresponding gaseous species.[39,40] Calculated total energies of halogen atoms were corrected to account for spin−orbit (SO) coupling using experimental spectroscopic data,[40] −1.61, −3.52, and −14.70 kJ mol^{-1}, for fluorine, chlorine, and bromine atoms, respectively. In the case of the diatomic radicals HgX, represented by the nondegenerate X $^2\Sigma$ state, the SO effect is zero;[41] the SO effect is also zero for HgX_2 molecules because they are closed shell systems. Results of previous theoretical calculations[31,32,36−38] are also presented in Table 2 for comparison purposes. These calculations have been performed at different levels of theory ranging from DFT to high-level correlated ab initio, however, in most cases moderate basis sets were employed that led to very high deviation of calculated energies from experiment. Similarly, in our calculations, B3LYP with the moderate LanL2DZ basis set reproduced reactions 3 and 6 enthalpies with a maximum error of ∼26 kJ mol^{-1}, while for recombination of HgX and X a deviation as large as 83 kJ mol^{-1} was observed. Apparently, the employed method was unable to recover the change in correlation energy for a nonisogyric[42] process

TABLE 2: Reaction Enthalpies (kJ mol^{-1}) Calculated at Different Levels of Theory; Spin−Orbit Correction for Halogen Atoms Is Included

		deviation from experiment ($\Delta_r H^{298}_{calc} - \Delta_r H^{298}_{exp}$)				
reaction	experiment[a]	previous calculations	B3LYP/ L2	B3LYP/ E60&AQZ	CCSD(T)/L2&G6// QCISD/L2&G6	CCSD(T)/E60&A5Z// QCISD/E60&G6
Hg + F → HgF	−137.84	−64.9,[b] 46.0,[c] −65.2[d]	−16.9	0.2	30.1	1.0 (9.5[e])
HgF + F → HgF_2	−375.97		61.2	4.9	−1.1	
Hg + F_2 → HgF_2	−355.03	12.1, [f] −5.7[g]	1.1	−3.8	12.8	
Hg + Cl → HgCl	−104.23	−25.2,[b] 33.9,[h] 46.3,[c] −24.7[d]	−5.6	15.0	24.9	6.9 (−0.6[e])
HgCl + Cl → $HgCl_2$	−346.05		85.4	32.5	15.3	
Hg + Cl_2 → $HgCl_2$	−207.67	42.7,[f] 75.4[i]	−21.5	27.2	14.4	
Hg + Br → HgBr	−69.06	−30.4[b]	−28.9	9.2	20.1	6.3 (0.8[e])
HgBr + Br → $HgBr_2$	−301.50		61.0	31.1	18.4	
Hg + Br_2 → $HgBr_2$	−177.74		−1.1	27.1	14.7	

[a] Ref 40. [b] LDF.[31] [c] QRPP−MP2.[32] [d] LDA.[32] [e] Calculated using extrapolation formula $E(L) = A + B \exp(-CL)$.[42] [f] BDF−R.[36] [g] QRPP−CCSD(T).[36] [h] CCI.[37] [i] CCI.[38]

represented by reaction 5, leading to poor results. The dissociation energies of molecular halogens were also significantly underestimated. Modifying eq 5 to conserve spin, i.e.,

$$HgX + X_2 \rightarrow HgX_2 + X \qquad (7)$$

and using the experimental atomization energy of X_2 (158.78, 242.60, and 192.81 kJ mol^{-1} for F_2, Cl_2, and Br_2),[40] reduced the enthalpy deviations to −17.1, 25.0, and −23.4 kJ mol^{-1}, for the reactions involving F, Cl, and Br, respectively. Using B3LYP with the ECP60MWB(9s9p6d4f) basis set for mercury and aug-cc-pVQZ for halogens significantly reduced the error in reaction 5 enthalpies, but had little effect on the enthalpies of reactions 3 and 6. Extending the basis set for halogens to aug-cc-pV5Z did not lead to a noticeable improvement in the reaction enthalpies, indicating that basis set convergence limit at this level of theory has been reached. Uneven performance of B3LYP has been reported in a recent study[43] on Hg/H_2O complexes where the quality of the results depended on whether the complex was neutral or cationic as well as on the geometry of the complex. Authors[43] mention that, in some cases, B3LYP geometries were intermediate between MP2 and QCISD, being closer to QCISD while in other cases they rather agreed with MP2 results. Thus, overall, the B3LYP method cannot be judged to be performing well, though it might be considered as an alternative to high-level ab initio methods in certain cases.

As Table 2 shows, high-level CCSD(T)//QCISD calculations with moderate LanL2DZ and 6-311G(2df) basis sets for mercury and halogens, respectively, only slightly improved the reaction energies, suggesting that a more extended basis set needs to be used. Therefore, we investigated how the deviation in reaction 3 energy depends on the quality of the basis set employing ECP60MWB(9s9p6d4f) for mercury and (aug)-cc-pV*N*Z (N = 3 to 6) for halogens. Extending the basis set for halogens, while keeping LanL2DZ for Hg, diverged the bonding energy away from experimental value. At the same time, as Figure 1 shows, using the ECP60MWB(9s9p6d4f) basis set for Hg in a similar calculation converged the bonding energy to a value close to experiment. As can be seen, using a basis set for halogens as large as aug-cc-pV5Z is necessary to reproduce the atomization energy of HgX to an absolute error less than 10 kJ mol^{-1}. A combination of E60 with A5Z is reasonably well balanced: 5.6 electrons per primitive for Hg and 12.4 electrons per primitive for Br, while in a similar combination of L2 with A5Z there are only 2.5 electrons per primitive for Hg and the resulting basis set is unbalanced. Extending the basis set for Hg, for example, to ECP60MWB(11s10p9d4f),[44] is expected to lead to more accurate results, but it would also make the calculation more computationally expensive. Extrapolation of the type $E(L) = A + B \exp(-CL)$, where L = 3, 4, 5, 6,[42] led to 9.7, 0.3, and 1.9 kJ mol^{-1} deviations at the infinite basis set limit in atomization energies for HgF, HgCl, and HgBr, respectively. The results of these high-level ab initio calculations were then used in the evaluation of rate constants for the reaction of mercury with halogen atoms (vide infra).

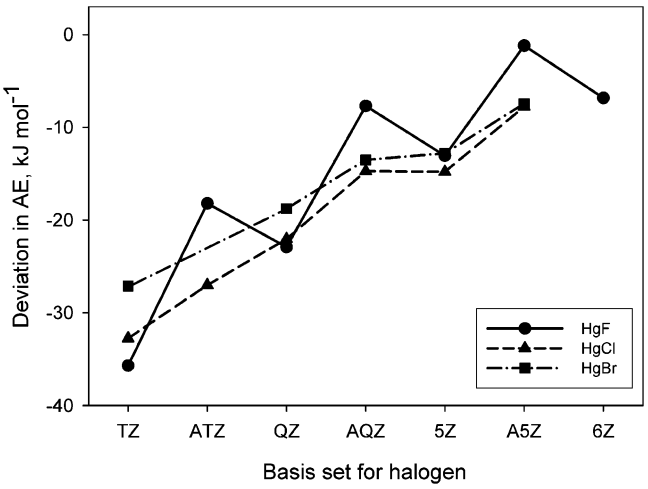

Figure 1. Basis set convergence of CCSD(T) atomization energies (*AE*) for HgX; the ECP60MWB(9s9p6d4f) basis set was employed for mercury.

3. Kinetics of Halogen−Mercury Atomic Recombination

3.1. Theoretical Models. Rate constant calculations were performed for the recombination of Hg and X considering the following sequence of elementary steps:

$$Hg + X \rightleftharpoons HgX^* \qquad (8)$$

$$HgX^* + M \rightarrow HgX + M \qquad (9)$$

The first step (reaction 8) accounts for the formation of the diatomic molecule HgX* from the separated atomic reactants. This molecule is primarily formed in an unbound excited vibrational state and may either be stabilized by a collision with a molecule of the bath gas (M) or dissociate back to the atomic reactants. If the pressure is high, the deactivation mechanism (reaction 9) is extremely fast and the overall rate constant for

recombination equals the rate constant for the first step. Conversely, if the bath gas pressure is low, the collisional deactivation mechanism may play an important role.

First, the high-pressure limit rate constants for the recombination of Hg and X were evaluated using collision theory;[45] then they were compared to the results of the Canonical Variational Transition State Theory (CVTST).[46]

The collision theory, based on the Langevin capture model,[47,48] defines the transition state (TS) at a given energy E with respect to the bottom of the reactant channel, by the position of the top of the centrifugal barrier. This effective potential barrier, created by an exact compensation of the centrifugal repulsive force and the attractive interaction force, is characterized by $r^{\ddagger}$, its position along the reaction coordinate, and L_{max}, the maximum value of the angular momentum compatible with the energy, through the two following conditions:

$$\begin{cases} V(r^{\ddagger},L_{max}) = \dfrac{{L_{max}}^2}{2\mu r^{\ddagger 2}} + V(r^{\ddagger}) = E \\ \left.\dfrac{\partial V(r,L_{max})}{\partial r}\right|_{r^{\ddagger}} = 0 \end{cases} \tag{10}$$

where μ is the diatomic molecule reduced mass, r is the interatomic distance, and $V(r)$ is the potential describing the interaction between the two atoms. The capture cross section $\sigma(E)$ is then calculated by

$$\sigma(E) = \pi {b_{max}}^2 \tag{11}$$

where b_{max}, the maximal impact parameter, is related to L_{max} by

$$b_{max} = \frac{L_{max}}{\sqrt{2\mu E}} \tag{12}$$

The high-pressure limit canonical rate constant is recovered by averaging the energy-resolved capture cross section over the relative kinetic energy distribution at a given temperature T,

$$k_{inf}(T) = \frac{1}{k_B T}\left(\frac{8}{\pi\mu k_B T}\right)^{1/2}\int_0^{\infty} E\sigma(E)\, e^{-k_B T}\, dE \tag{13}$$

where k_B is the Boltzmann constant.

For the calculation of the CVTST rate constant, the equilibrium constant K_{eq} and the high-pressure limit for the rate of unimolecular decomposition $k^{CVT}(T)$ were first evaluated and then the rate constant for recombination was evaluated. The unimolecular rate constant, $k^{CVT}(T)$, is calculated at a fixed temperature by minimizing the generalized rate constant, $k^{GT}(T, r)$, with respect to r, which defines the dividing surface.[46]

The deactivation process (reaction 9) was treated by a simple model similar to the one developed by Bunker,[49] within the framework of the capture model. The vibrationally excited diatomic molecule, HgX*, is supposed to be stabilized if it collides with a bath gas molecule during its lifetime. At given energy E and angular momentum L, this lifetime is approximated by one period of vibration, which is defined by

$$\tau(E,L) = 2\int_{r^-}^{r^{\ddagger}}\left\{\frac{2}{\mu}\left(E - \frac{L^2}{2\mu r^2} - V(r)\right)\right\}^{-1/2} dr \tag{14}$$

where $r^{\ddagger}$ is the position of the transition TS (see eq 10), and r^- is determined by the integrand condition of existence. The range between $r^{\ddagger}$ and r^- defines arbitrarily the configuration domain for which HgX* is considered as a molecular entity able to be stabilized. For $r > r^{\ddagger}$, Hg and X are considered as separated atoms. The average lifetime for a given energy E is then given by

$$\tau(E) = \frac{1}{L_{max}}\int_0^{L_{max}} \tau(E,L)\, dL \tag{15}$$

The collision frequency Z of HgX* with the bath gas molecules (here N_2 and O_2) is approximated by

$$Z = 0.8Z_{N_2} + 0.2Z_{O_2} \tag{16}$$

where Z_{N_2} or Z_{O_2} are, respectively, the collision frequencies of HgX* with N_2 and O_2. This average takes into account the chemical composition of the bath gas. For a given pressure P and temperature T, Z_{O_2} and Z_{N_2} are estimated, within the framework of the hard-sphere collision model.[50] In this calculation, the overall size d of each molecule, determined by adding the bond length r_e and the van der Waals radii r_{vdw} of each atom forming the molecule, is considered. The parameters used are summarized in Table 3.

Thus, for a given energy E, the deactivation probability $P(E)$ for an excited diatomic molecule HgX* is given by

$$P(E) = Z\tau(E) \tag{17}$$

In this simple model, each collision leads to deactivation and the maximum value of $P(E)$ is one. Then, the capture cross section taking into account deactivation, $\sigma_{de}(E)$, at energy E is now given by

$$\sigma_{de}(E) = \pi {b_{max}}^2 P(E) \tag{18}$$

The corresponding pressure-dependent thermal rate constant $k_P(T)$ is recovered by averaging the previous capture cross section $\sigma_{de}(E)$ over the relative kinetic energy distribution, i.e., using eq 13 with $\sigma_{de}(E)$ instead of $\sigma(E)$.

TABLE 3: Atomic and Molecular Parameters Used in the Rate Constant Calculations

atom	r_{vdw}[a], Å	
F	1.47	
Cl	1.75	
Br	1.85	
N	1.55	
O	1.52	
Hg	1.55	
molecule	**r_e, Å**	**d, Å**
HgF	2.048	5.068
HgCl	2.433	5.733
HgBr	2.580	5.980
N_2	1.1	4.2
O_2	1.2	4.2

[a] Ref 60.

3.2. Calculated Rate Constants and Their Implications. Table 4 presents the calculated high-pressure limit rate constants $k_{inf}(T)$ and the pressure-dependent thermal rate constants $k_P(T)$ for the recombination of atomic halogens with mercury. The Morse function was used in the collision theory and VTST calculations to describe the Hg−X interaction potential. The function parameters were obtained by fitting eq 19 to the Hg−X energies at different separations calculated at the CCSD(T)/E60&AQZ level of theory:

$$V(r) = D_e\{1 - \exp(-\beta(r - r_e))\}^2 \tag{19}$$

TABLE 4: Comparison of Calculated and Experimental Dissociation Energies (kJ mol^{-1}) for HgX

	D_e	D_0^0		
species	this work	this work[a]	Gaydon[b]	Huber and Herzberg[c]
HgF	136.65	133.74	133.89	173.61
HgCl	96.45	94.79	96.23	96.45
HgBr	61.62	60.53	67.52	68.48

[a] $D_0^0 = D_e - \mathrm{ZPE(HgX)}$. [b] Ref 51. [c] Ref 52.

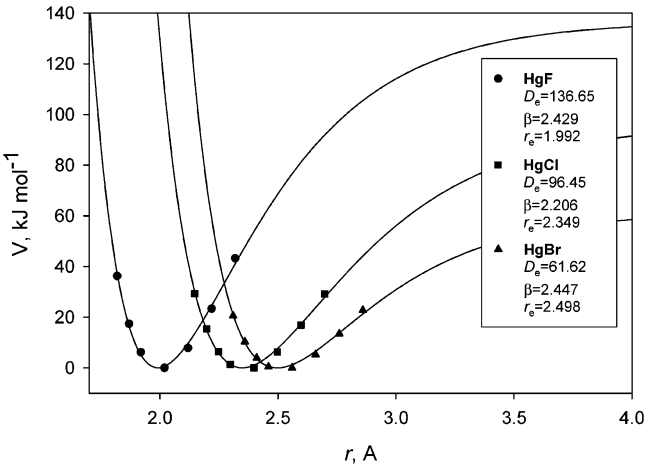

Figure 2. HgX energy potentials calculated at the CCSD(T)/MWB60ECP&AV5Z theory level. Lines were plotted by fitting Morse function to the ab initio data; a spin−orbit correction was applied to the dissociation energy.

where D_e is the dissociation energy (kJ mol^{-1}), r_e is the equilibrium bond distance (Å), and parameter β is (Å^{-1}). Figure 2 displays the calculated fits to the high-level ab initio data as well as the corresponding Morse parameters. The procedure involved keeping D_e constant while varying r_e and β to obtain the best fit to the ab initio data. One can see that at intermediate separations between Hg and X, explicit treatment of spin−orbit coupling for each point on the ab initio interaction potential would be necessary. Indeed, upon complete dissociation, the HgX radical, having X $^2\Sigma^+$ electronic state, is transformed into atoms Hg and Br represented by $^1S_0$ and $^2P_{3/2}$ terms, respectively. Correspondingly, the SO contribution to the interaction potential due to the Hg...X complex changes from zero at equilibrium, since HgX (X $^2\Sigma^+$) is nondegenerate,[41] to −1.61, −3.52, or −14.70 kJ mol^{-1} for halogen atom, at infinite separation between Hg and X. Around the equilibrium geometry at $|r-r_e| < 0.5$ Å, the Hg...X collision complex resembles the HgX moiety rather than the separate atoms Hg and X. Thus, only the energies at moderate separations were used in the fitting procedure when it was safe to assume that the X $^2\Sigma^+$ electronic state for the Hg...X complex is preserved and the SO effect is zero. At the same time, the dissociation energies of HgX were corrected for the spin−orbit coupling due to halogen atoms. Table 4 compares the calculated dissociation energies used in eq 19 with the available experimental values from Gaydon[51] and Huber and Herzberg.[52] These experimental data are very close to each other except for HgF where Herzberg's value[52] is 0.4 eV higher and listed as having high uncertainty. It should be noted, however, that changing the dissociation energy slightly would not substantially affect the kinetic data. The high-pressure rate constant depends only on the part of the potential between infinity and the top of the centrifugal barrier. This part is not expected to change significantly with a slight change in the dissociation energy; it would only affect the lifetime calculated by eq 14, but not in a radical way.

Using two different approaches, CVTST and the capture model, resulted in consistent values of the high-pressure-limit rate constants, though, for a given T, the CVTST rate constant was greater than the rate constant calculated using the capture model. This is not surprising since in the transition state theory, the better the TS is defined, the lower is the calculated rate constant.[53] In the former theory the TS is defined as the best canonical average dividing surface, whereas in the latter it is defined in a more rigorous way, for each energy.

Table 5 shows that the calculated pressure-dependent rate constant k_p for the reaction of mercury with chlorine atoms is below the available experimental values, 1.5×10^{-11} and 1.0×10^{-11} cm^3 molecule^{-1} s^{-1}, within factors of 5.3 and 3.6. The experimental data were obtained using time-resolved[19] and relative rate[10] techniques, respectively. At the same time, k_p for the reaction of mercury with atomic bromine is very close to the recent experimental value, 3.2×10^{-12} cm^3 molecule^{-1} s^{-1}.[10] Since k_p revealed a weak negative temperature dependence, quite typical for a simple atomic recombination, one may expect the reaction to accelerate slightly in the Arctic troposphere, where the temperature is known to drop to about 233 ± 10 K in the springtime.

The results of the present model for deactivation, where each collision is supposed to deactivate the unbound excited vibrational state, could certainly be improved by incorporating a collision efficiency factor.[54] Nevertheless, such an improvement is not expected to change the calculated rate constants significantly. As a consequence, the simple model proposed here captures the main features of diatomic recombination kinetics and leads to a consistent comparison with experiments.

One can see that the reactions of Hg with atomic halogens are considerably fast, and it is very likely that they, with the exception of the reaction with atomic fluorine whose concentration in the troposphere is negligibly low, may contribute to the chemistry of mercury in the gas phase. We evaluated the lifetime of Hg due to loss reactions with chlorine and bromine atoms to be almost two years and half a day respectively, assuming Cl and Br steady-state concentrations to be 10^4 and 10^7 atom cm^{-3}.[11,55] Hence, despite the fast rate coefficient of the Cl-atom-initiated reaction of mercury, the inferred concentration of chlorine atoms is far too low to play a significant role. Atomic bromine, however, is present in a high enough concentration to completely destroy mercury within a short period of time, as observed in the Arctic. Nevertheless, further research is needed to assess the contribution from other active species such as halogen oxides to draw a complete picture of the mercury chemistry in the troposphere.

TABLE 5: Calculated Kinetic Parameters for Recombination of Halogen Atoms with Mercury

	VTST	collision theory			
reaction	k_{inf}(298 K) × 10^{10}, cm^3 molecule s^{-1}	Z(1 atm, 298K) × 10^{-9}, s^{-1}	k_{inf}(298 K) × 10^{10}, cm^3 molecule s^{-1}	k_p(1 atm, 298 K) × 10^{12}, cm^3 molecule s^{-1}	k_p(1 atm, T), cm^3 molecule s^{-1}
Hg + F → HgF	4.69	8.24	4.29	1.86	0.92×10^{-12} exp(206.81/T)
Hg + Cl → HgCl	4.32	9.41	3.93	2.81	1.38×10^{-12} exp(208.02/T)
Hg + Br → HgBr	2.75	9.52	2.33	2.07	1.01×10^{-12} exp(209.03/T)

Acknowledgment. We acknowledge financial support from NSERC (National Science and Engineering Research Council of Canada), Environment Canada, C^{2}GCR (the Centre for Climate and Global Change Research, McGill University). We thank the Centre for Research in Molecular Modeling (CERMM) at Concordia University for computer time. A.F.K. acknowledges NSERC/NATO Postdoctoral Science Program for financial support. P.L. acknowledges the Centre for Research in Molecular Modeling (CERMM), Concordia University, and the Fonds pour la Formation des Chercheurs et l'Aide a la recherche (FCAR), for providing his postdoctoral financial support.

References and Notes

(1) Lindberg, S. E.; Stratton, W. J. *Environ. Sci. Technol.* **1998**, *32*, 49.
(2) Schroeder, W. H.; Yarwood, G.; Niki, H. *Water, Air, Soil Pollut.* **1991**, *56*, 653.
(3) Schroeder, W. H.; Anlauf, K. G.; Barrie, L. A.; Lu, J. Y.; Steffen, A.; Schneeberger, D. R.; Berg, T. *Nature* **1998**, *394*, 331.
(4) Schroeder, W. H.; Barrie, L. A. *IGAC Newsletter* **1998**, 7.
(5) Tokos, J. J. S.; Hall, B.; Calhoun, J. A.; Prestbo, E. M. *Atmos. Environ.* **1998**, *32*, 823.
(6) P'yankov, V. A. *Zh. Obsch. Khim. (Russ. J. Gen. Chem.)* **1949**, *19*, 224.
(7) Hall, B. *Water, Air, Soil Pollut.* **1995**, *80*, 301.
(8) Skare, I.; Johansson, R. *Chemosphere* **1992**, *24*, 1633.
(9) Medhekar, A. K.; Rokni, M.; Trainor, D. W.; Jacob, J. H. *Chem. Phys. Lett.* **1979**, *65*, 600.
(10) Ariya, P. A.; Khalizov, A.; Gidas, A. *J. Phys. Chem. A* **2002**, *106*, 7310.
(11) Ariya, P. A.; Jobson, B. T.; Sander, R.; Niki, H.; Harris, G. W.; Hopper, J. F.; Anlauf, K. G. *J. Geophys. Res.* **1998**, *103*, 13169.
(12) Barrie, L.; Platt, U. *Tellus, Ser. B* **1997**, *49B*, 450.
(13) Langendorfer, U.; Lehrer, E.; Wagenbach, D.; Platt, U. *J. Atmos. Chem.* **1999**, *34*, 39.
(14) Martinez, M.; Arnold, T.; Perner, D. *Ann. Geophys.* **1999**, *17*, 941.
(15) Mueller, R.; Crutzen, P. J.; Grooss, J.-U.; Bruehl, C.; Russell, J. M., III.; Tuck, A. F. *J. Geophys. Res.* **1996**, *101*, 12531.
(16) Ramacher, B.; Rudolph, J.; Koppmann, R. *J. Geophys. Res.* **1999**, *104*, 3633.
(17) Khalizov, A.; Viswanathan, B.; Ariya, P. A. Unpublished data.
(18) Shepler, B. C.; Peterson, K. A. *J. Phys. Chem. A* **2003**, *107*, 1783.
(19) Horne, D. G.; Gosavi, R.; Strausz, O. P. *J. Chem. Phys.* **1968**, *48*.
(20) Frisch, M. J.; Trucks, G. W.; Schlegel, H. B.; Scuseria, G. E.; Robb, M. A.; Cheeseman, J. R.; Zakrzewski, V. G.; Montgomery, J. A., Jr.; Stratmann, R. E.; Burant, J. C.; Dapprich, S.; Millam, J. M.; Daniels, A. D.; Kudin, K. N.; Strain, M. C.; Farkas, O.; Tomasi, J.; Barone, V.; Cossi, M.; Cammi, R.; Mennucci, B.; Pomelli, C.; Adamo, C.; Clifford, S.; Ochterski, J.; Petersson, G. A.; Ayala, P. Y.; Cui, Q.; Morokuma, K.; Malick, D. K.; Rabuck, A. D.; Raghavachari, K.; Foresman, J. B.; Cioslowski, J.; Ortiz, J. V.; Baboul, A. G.; Stefanov, B. B.; Liu, G.; Liashenko, A.; Piskorz, P.; Komaromi, I.; Gomperts, R.; Martin, R. L.; Fox, D. J.; Keith, T.; Al-Laham, M. A.; Peng, C. Y.; Nanayakkara, A.; Gonzalez, C.; Challacombe, M.; Gill, P. M. W.; Johnson, B.; Chen, W.; Wong, M. W.; Andres, J. L.; Gonzalez, C.; Head-Gordon, M.; Replogle, E. S.; Pople, J. A. *Gaussian 98*, Revision A.7; Gaussian, Inc.: Pittsburgh, PA, 1998.
(21) Hay, P. J.; Wadt, W. R. *J. Chem. Phys.* **1985**, *82*, 270.
(22) Hay, P. J.; Wadt, W. R. *J. Chem. Phys.* **1985**, *82*, 299.
(23) Wadt, W. R.; Hay, P. J. *J. Chem. Phys.* **1985**, *82*, 284.
(24) Andrae, D.; Haeussermann, U.; Dolg, M.; Stoll, H.; Preuss, H. *Theor. Chim. Acta* **1990**, *77*, 123.
(25) Schwerdtfeger, P.; Wesendrup, R. http://www.theochem.uni-stuttgart.de/pseudopotentials/index.en.html, 1999.
(26) Dunning, T. H., Jr. *J. Chem. Phys.* **1989**, *90*, 1007.
(27) Woon, D. E.; Dunning, T. H., Jr. *J. Chem. Phys.* **1993**, *98*, 1358.
(28) Wilson, A. K.; Woon, D. E.; Peterson, K. A.; Dunning, T. H., Jr. *J. Chem. Phys.* **1999**, *110*, 7667.
(29) Wilson, A.; van Mourik, T.; Dunning, T. H., Jr. *THEOCHEM* **1997**, *388*, 339.
(30) Cundari, T. R.; Yoshikawa, A. *J. Comput. Chem.* **1998**, *19*, 902.
(31) Liao, M.-S.; Zhang, Q.-E.; Schwarz, W. H. E. *Inorg. Chem.* **1995**, *34*, 5597.
(32) Schwerdtfeger, P.; Boyd, P. D. W.; Brienne, S.; McFeaters, J. S.; Dolg, M.; Liao, M. S.; Schwarz, W. H. E. *Inorg. Chim. Acta* **1993**, *213*, 233.
(33) Kaupp, M.; Vonschnering, H. G. *Inorg. Chem.* **1994**, *33*, 4179.
(34) Kaupp, M.; Dolg, M.; Stoll, H.; Vonschnering, H. G. *Inorg. Chem.* **1994**, *33*, 2122.
(35) Kaupp, M.; Vonschnering, H. G. *Inorg. Chem.* **1994**, *33*, 2555.
(36) Liu, W.; Franke, R.; Dolg, M. *Chem. Phys. Lett.* **1999**, *302*, 231.
(37) Stroemberg, D.; Stroemberg, A.; Wahlgren, U. *Water, Air, Soil Pollut.* **1991**, *56*, 681.
(38) Stroemberg, D.; Gropen, O.; Wahlgren, U. *Chem. Phys.* **1989**, *133*, 207.
(39) Lide, D. R. *CRC Handbook of Chemistry and Physics*, 81st ed.; CRC Press: Boca Raton, FL, 2000.
(40) Chase, M. W., Jr. *J. Phys. Chem. Ref. Data* **1998**, *Monograph 9*, 1.
(41) Herzberg, G. *Molecular Spectra and Molecular Structure. 1. Spectra of Diatomic Molecules*, 2nd ed.; Van Nostrand Reinhold Company: Toronto, 1950.
(42) Jensen, F. *Introduction to Computational Chemistry*; John Wiley & Sons: New York, 1999.
(43) Soldan, P.; Lee, E. P. F.; Wright, T. G. *J. Phys. Chem. A* **2002**, *106*, 8619.
(44) Wesendrup, R.; Kloo, L.; Schwerdtfeger, P. *Int. J. Mass Spectrom.* **2000**, *201*, 17.
(45) Steinfeld, J. I.; Francisco, J. S.; Hase, W. L. *Chemical Kinetics and Dynamics*; Prentice Hall: Upper Saddle River, NJ, 1999.
(46) Kreevoy, M. M.; Truhlar, D. G. Transition State Theory. In *Investigation of Rates and Mechanisms of Reactions*; Bernasconi, C. F., Ed.; Wiley: New York, 1986; Vol. 6, p 14.
(47) Levine, R. D.; Bernstein, R. B. *Molecular Reaction Dynamics and Chemical Reactivity*; Oxford University Press: Oxford, 1987.
(48) Light, J. C. *J. Chem. Phys.* **1964**, *40*, 3221.
(49) Bunker, D. L. *J. Chem. Phys.* **1960**, *32*, 1001.
(50) Levine, I. N. *Physical Chemistry*; McGraw-Hill: New York, 1988.
(51) Gaydon, A. G. *Dissociation Energies and Spectra of Diatomic Molecules*, 2nd ed., revised ed.; Chapman and Hall: London, 1953.
(52) Huber, K.-P.; Herzberg, G. *Constants of diatomic molecules*; Van Nostrand Reinhold: New York, Toronto, 1979.
(53) Truhlar, D. G.; Garrett, B. C.; Klippenstein, S. J. *J. Chem. Phys.* **1996**, *100*, 12771.
(54) Gilbert, S. C. S. *Theory of unimolecular and recombination reactions*; Blackwell: Cambridge, MA, 1990.
(55) Jobson, B. T.; Niki, H.; Yokouchi, Y.; Bottenheim, J.; Hopper, F.; Leaitch, R. *J. Geophys. Res., [Atmos.]* **1994**, *99*, 23.
(56) Givan, A.; Loewenscuss, A. *J. Chem. Phys.* **1980**, *72*, 3809.
(57) Gregg, A. H.; Hampson, G. C.; Jenkins, G. I.; Jones, P. L. F.; Sutton, L. E. *Trans. Faraday Soc.* **1937**, *33*, 852.
(58) Aylett, B. J. *Comprehensive Inorganic Chemistry*; Pergamon Press: Elmsford, NY, 1973; Vol. 3.
(59) Adams, D. M.; Hills, D. J. *J. Chem. Soc., Dalton Trans.* **1978**, 776.
(60) Bondi, A. *J. Phys. Chem.* **1964**, *68*, 441.